

# Constraining the Polarized Gluon Distribution Function of the Proton with Recent STAR Measurements

Nicholas LUKOW<sup>1\*</sup>

<sup>1</sup>Temple University, Philadelphia, PA 19122 USA

E-mail: [nicholas.lukow@temple.edu](mailto:nicholas.lukow@temple.edu)

(Received January 15, 2022)

The contribution of the gluon spin to the spin of the proton is being studied through the use of the unique capability of the Relativistic Heavy Ion Collider (RHIC) to collide longitudinally polarized protons at  $\sqrt{s} = 200$  GeV and  $\sqrt{s} = 510$  GeV. The kinematic coverage of the Solenoidal Tracker At RHIC (STAR) allows access to gluons through quark-gluon and gluon-gluon scattering processes which dominate particle production at low and medium transverse momentum. The polarized gluon distribution function,  $\Delta g(x)$ , can be constrained through global analyses of the longitudinal double-spin asymmetries ( $A_{LL}$ ) of inclusive jet and di-jet production. Published inclusive jet results from 2009 data at mid-rapidity ( $|\eta| < 1$ ) at  $\sqrt{s} = 200$  GeV have been included in global analyses and suggest a significant non-zero truncated first moment of  $\Delta g(x)$  for  $x > 0.05$ . An additional data sample of  $52 \text{ pb}^{-1}$  has been collected in 2015 at the same collision energy. This new data sample is over twice as large as the previous sample, providing an opportunity to improve the precision of  $\Delta g(x)$  for  $x > 0.05$ . The published results from the analysis of the 2015 data are presented along with the status of the analysis using an even larger data sample of  $250 \text{ pb}^{-1}$  collected at  $\sqrt{s} = 510$  GeV in 2013.

**KEYWORDS:** gluon helicity, proton spin decomposition, jet, di-jet

## 1. Introduction

In 1988 results from the European Muon Collaboration showed that the intrinsic spins of the quarks contribute little to the proton spin [1]. Recent measurements have shown that the first moment of the polarized quark distribution,  $\Delta\Sigma$ , is approximately 0.25 [2]. The remaining contribution must then come from the combination of the intrinsic spins of the gluons and the orbital angular momenta of the quarks and gluons. One of the primary goals of the RHIC spin program is to perform high precision measurements to constrain the polarized gluon distribution function,  $\Delta g(x)$ , of the proton.

RHIC is the only collider capable of colliding polarized proton beams with center-of-mass energies up to 510 GeV, making it a unique tool for probing the spin structure of the proton. The measurements described here are carried out with STAR. The STAR detector subsystems used for these analyses include the Time Projection Chamber (TPC), Barrel and Endcap Electromagnetic Calorimeters (BEMC/EEMC), Vertex Position Detector (VPD), and Zero Degree Calorimeter (ZDC). The TPC provides tracking and covers  $|\eta| < 1.3$  in pseudorapidity with full azimuthal coverage. The electromagnetic calorimeters, which cover  $-1 < \eta < 2$  and  $2\pi$  in azimuth, are used to trigger on high momentum particles (photons/electrons/ $\pi^0$ ) and to measure the neutral component of jets. The VPD and ZDC are used to measure the relative luminosity [3].

---

\*For the STAR collaboration

## 2. Gluon Polarization Measurements

At RHIC,  $gg$  and  $qg$  scatterings dominate jet production at low and medium transverse momenta ( $p_T$ ) making jet production sensitive to the gluon distribution. The polarized gluon distribution can be probed by measuring the longitudinal double-spin asymmetry ( $A_{LL}$ ) of jets. Jets are reconstructed with charged TPC tracks and EMC energy deposits using the anti- $k_t$  algorithm [4]. Details on the jet and di-jet selection criteria can be found in [5].

Many STAR results which have been published [6–8] have been included in global analyses which suggest a non-zero gluon polarization [9–11]. There is still a need to increase the precision of these measurements, and to extend the sampled partonic momentum fraction,  $x$ , to lower values.

### 2.1 Inclusive Jets

The first STAR results to show strong evidence of a non-zero gluon polarization were the inclusive jet  $A_{LL}$  results from polarized proton-proton collisions at  $\sqrt{s} = 200$  GeV collected in 2009 [6]. The measured asymmetry was consistently larger than the values predicted by global fits at the time, though within the theory uncertainty bands. In 2014, the 2009 inclusive jet results were included in global analyses, and the resulting truncated first moment of  $\Delta g(x)$  reported by the NNPDF and DSSV collaborations were  $\Delta G = \int_{0.05}^{0.2} \Delta g(x) dx = 0.17 \pm 0.06$  [9] and  $\Delta G = \int_{0.05}^1 \Delta g(x) dx = 0.19 \pm 0.06$  [10], respectively.

The uncertainties at low  $x$  are still large, and more data are needed to constrain  $\Delta g(x)$  in that region. In 2012 and 2013 RHIC delivered proton-proton collisions at  $\sqrt{s} = 510$  GeV, corresponding to integrated luminosities of  $82 \text{ pb}^{-1}$  and  $250 \text{ pb}^{-1}$  respectively. The higher center-of-mass energy provides greater sensitivity to lower momentum fractions ( $x > 0.015$ ) than the 200 GeV data.

Collection of longitudinally polarized data concluded in 2015 after more data was recorded at  $\sqrt{s} = 200$  GeV to corroborate the 2009  $A_{LL}$  results with increased precision. The 2015 data sample has an integrated luminosity of  $52 \text{ pb}^{-1}$ , over twice as much as the 2009 sample. The measured inclusive jet  $A_{LL}$  for the 2012 [5], 2013 [12], and 2015 [13] data samples can be seen in Fig. 1 plotted alongside the values for the 2009 data sample.

A Monte Carlo sample embedded in zero bias data is used to quantify systematic uncertainties. DSSV14 global fits are used in the Monte Carlo sample for estimating systematic effects such as trigger and reconstruction bias. The underlying event subtraction technique, developed in [14], was adapted in analyses that followed the 2009 inclusive jet results, leading to improved systematic uncertainties for jet  $p_T$  and di-jet  $M_{inv}$ .

### 2.2 Di-Jets

Di-jets can probe narrower regions in sampled momentum fraction compared to inclusive jets (Fig. 2) providing additional constraints on the functional form of  $\Delta g(x)$ . The first di-jet results using the 2009 data investigated mid-rapidity di-jets ( $-0.8 < \eta < 0.8$ ) and the results agree well with expectations from the 2014 global fits [7]. The study was replicated with the additional  $\sqrt{s} = 200$  GeV data collected in 2015 and the results are consistent and have improved uncertainties (Fig. 3) [13]. Another study using the 2009 data utilized the endcap region of the STAR detector to analyze di-jets at intermediate rapidities, providing sensitivity to even lower momentum fractions. In the intermediate-rapidity di-jet analysis at least one jet in the di-jet pair was reconstructed in the endcap region ( $0.8 < \eta < 1.8$ ) [8]. The results of the intermediate-rapidity di-jet analysis agree well with the 2014 global fits except in the most forward topology bin (both jets in the endcap) where the results are above the fits but consistent within large uncertainties (Fig. 4). The DSSV collaboration recently included all the 2009 di-jet  $A_{LL}$  measurements in a Monte Carlo reweighting analysis, resulting in an increase in the gluon polarization for  $0.05 \lesssim x \lesssim 0.2$  and an improvement of the uncertainty in the high- $x$  region [11].

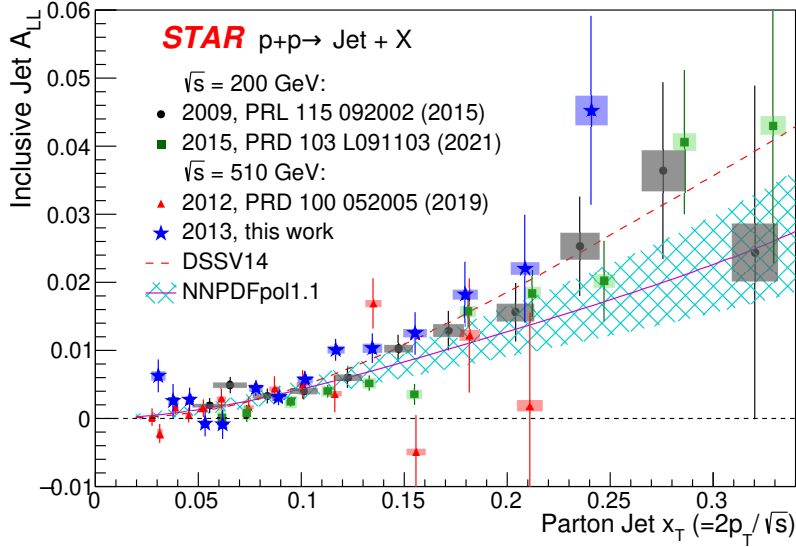


**Fig. 1.** Inclusive jet  $A_{LL}$  for the 2009 (black) [6], 2012 (red) [5], 2013 (blue) [12], and 2015 (green) [13] data samples plotted versus parton jet  $x_T$ . The vertical bars represent the statistical uncertainties and the shaded boxes represent the systematic uncertainties. Figure from [12].

Di-jet analyses were also performed using the 2012 and 2013  $\sqrt{s} = 510$  GeV data. For the mid-rapidity di-jet analysis, the sample was classified into additional topology configurations to sample different regions in  $x$  compared to the 2009 analysis. The final results of the 2012 and 2013 mid-rapidity  $A_{LL}$  analyses can be seen in Fig. 5. These results will provide new constraints on  $\Delta g(x)$  at a lower  $x$  region,  $x > 0.015$ , after being included in global analyses. Preliminary results of the intermediate-rapidity di-jet analyses of the 2012 and 2013 data have been released and the analyses are being finalized, and the intermediate-rapidity di-jet analysis of the 2015 data is currently underway.

### 3. Summary

The STAR collaboration has performed measurements of inclusive jet and di-jet  $A_{LL}$  at  $\sqrt{s} = 200$  and 510 GeV. The STAR 2009 inclusive jet results at 200 GeV were the first to show evidence of a non-zero gluon polarization. The 2015 inclusive jet results are consistent with the previous 2009 inclusive jet results, but with increased precision, providing further evidence of positive gluon polarization for  $x > 0.05$ . The 2015 mid-rapidity di-jet results are consistent with the 2009 mid-rapidity di-jet results and the latter has been used to improve the DSSV global fits using a Monte Carlo sampling approach. The 2012 and 2013 inclusive jet results at 510 GeV are also consistent with the 2009 results at 200 GeV, but provide better sensitivity to lower values of  $x$ . These results will provide important new constraints on  $\Delta g(x)$  especially for  $x < 0.05$ . The new 2012 and 2013 di-jet results will also provide important new constraints on the functional form of  $\Delta g(x)$  since measurements of  $A_{LL}$  for different di-jet topology configurations are sensitive to different regions in  $x$ . The inclusion of the recently published results in future global analyses will further constrain gluon polarization in the region  $0.015 \lesssim x \lesssim 0.5$ . The need for more data at lower values of  $x$  motivates the future Electron Ion Collider [15].

### References

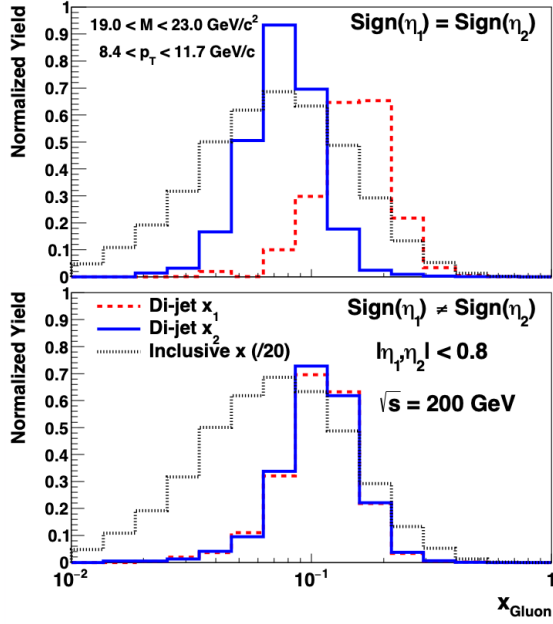


**Fig. 2.** Distribution of the values of gluon  $x_1$  and  $x_2$  from Pythia simulation for the same-sign topology, where the two jets have the same sign of jet  $\eta$  (upper panel), and for opposite-sign topology, where the two jets have the opposite sign of jet  $\eta$  (lower panel). Also shown is the  $x$  distribution for inclusive jets, scaled by a factor of 20. Figure from [7].

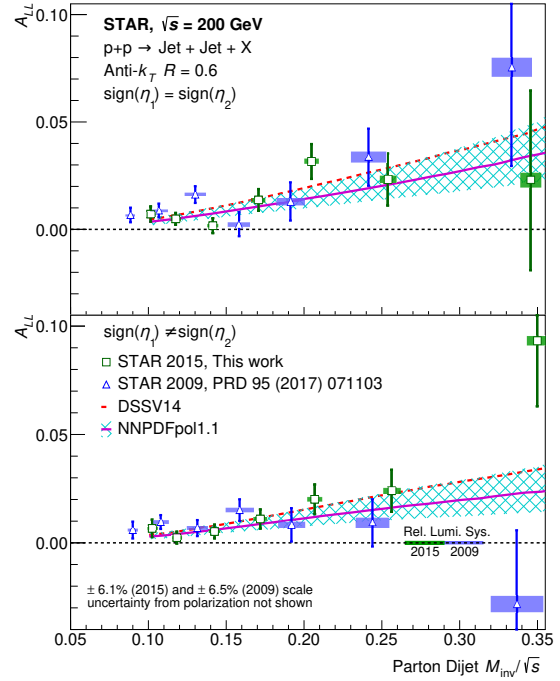


**Fig. 3.** Mid-rapidity di-jet  $A_{LL}$  plotted vs parton dijet invariant mass for two different di-jet event topologies from the 2009 and 2015 data samples. Figure from [13].

- [1] J. Ashman et al. [European Muon Collaboration] Phys. Lett. B 206 (2), 364 (1988).
- [2] C. A. Aidala, S. D. Bass, D. Hasch and G. K. Mallot, Rev. Mod. Phys. 85, 655 (2013).
- [3] K. Ackermann et al. [STAR Collaboration], Nucl. Instr. & Meth. A 499 624 (2003).
- [4] M. Cacciari, G. P. Salam, and G. Soyez, JHEP 04, 063 (2008).
- [5] J. Adam et al. [STAR Collaboration], Phys. Rev. D 100, 052005 (2019).
- [6] L. Adamczyk et al. [STAR Collaboration], Phys. Rev. Lett. 115, 092002 (2015).
- [7] L. Adamczyk et al. [STAR Collaboration], Phys. Rev. D 95, 071103(R) (2017).
- [8] J. Adam et al. [STAR Collaboration], Phys. Rev. D 98, 032011 (2018).
- [9] E. R. Nocera et al. [NNPDF Collaboration], Nucl. Phys. B 887, 276 (2014).
- [10] D. de Florian, R. Sassot, M. Stratmann and W. Vogelsang, Phys. Rev. Lett. 113, 012001 (2014).
- [11] D. de Florian, G. A. Lucero, R. Sassot, M. Stratmann and W. Vogelsang, Phys. Rev. D 100, 114027 (2019).
- [12] M.S. Abdallah et al. [STAR Collaboration] (2021) [hep-ex/2110.11020].
- [13] M.S. Abdallah et al. [STAR Collaboration], Phys. Rev. D 103, 091103 (2021).
- [14] B. Abelev et al. [ALICE Collaboration], Phys. Rev. D 91, 112012 (2015).
- [15] A. Accardi et al., Eur. Phys. J. A 52, 268 (2016).

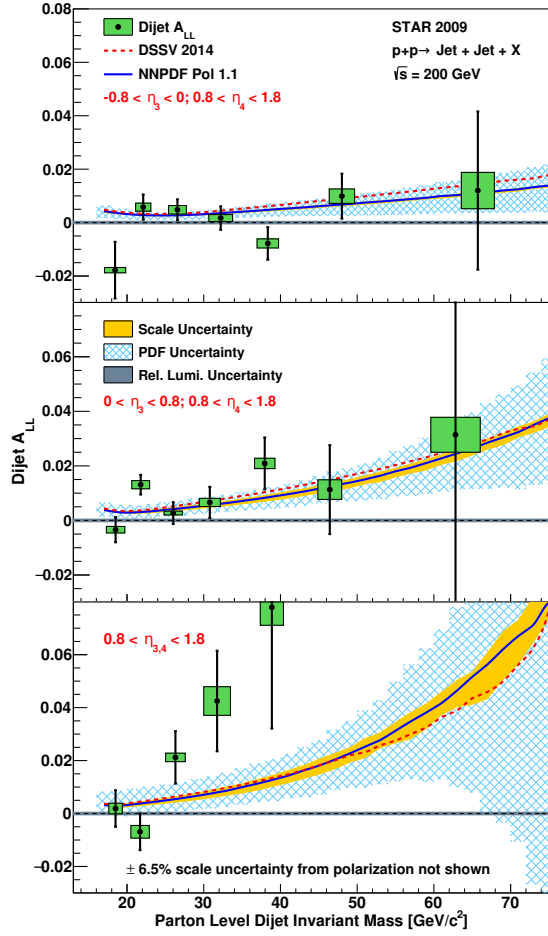


**Fig. 4.** Intermediate-rapidity di-jet  $A_{LL}$  plotted vs parton di-jet invariant mass for three different di-jet event topologies from the 2009 data sample. Figure from [8].

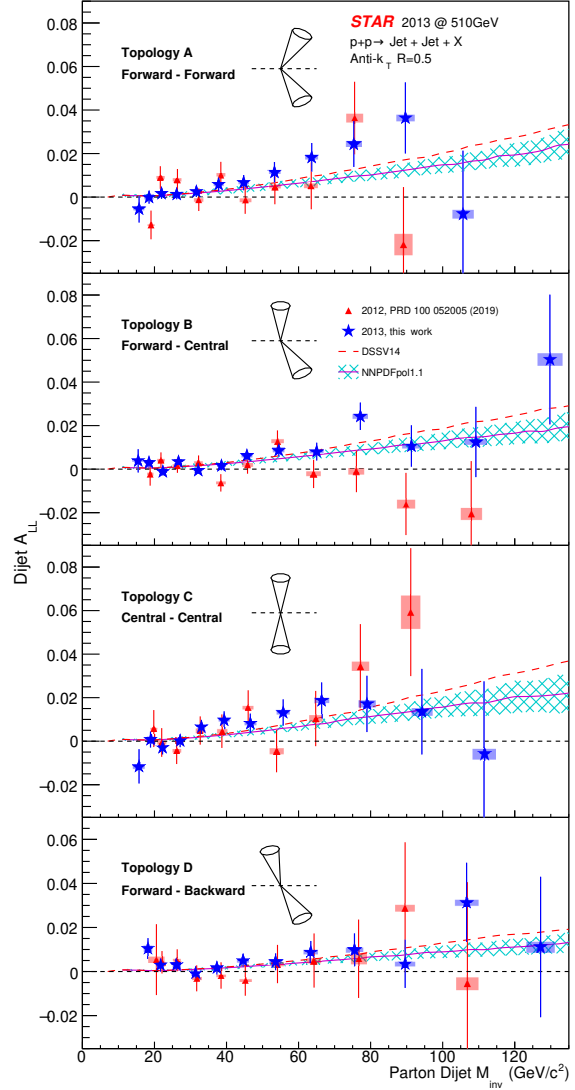


**Fig. 5.** Mid-rapidity di-jet  $A_{LL}$  plotted vs parton di-jet invariant mass for four different di-jet event topologies from the 2012 and 2013 data samples. Figure from [12].